Proc. VI Serbian-Bulgarian Astronomical Conference, Belgrade 7-11 May 2008,
Eds. M. S. Dimitrijević, M. Tsvetkov, L. Č. Popović, V. Golev
Publ. Astr. Soc. "Rudjer Bošković", No. 9, 2009, 233-243

OPTICAL OBSERVATIONS OF THE GALACTIC SUPERNOVA REMNANTS: G59.5+0.1, G84.9+0.5 AND G67.7+1.8

AYTAP SEZER[1,2], FATMA GÖK[2], ZEKI ASLAN[3], EBRU AKTEKIN[2], ENISE NIHAL ERCAN[1]

[1]*Boğaziçi University, Physics Department, Bebek-Istanbul 34342 - Turkey*
e-mail: aytap.sezer@boun.edu.tr; ercan@boun.edu.tr
[2]*Akdeniz University, Faculty of Art and Sciences, Department of Physics Antalya, 07058, Turkey*
e-mail: gok@akdeniz.edu.tr, eaktekin@akdeniz.edu.tr
[3]*Kültür University, Faculty of Art and Sciences, Department of Physics Istanbul, 34510, Turkey*
e-mail: z.aslan@iku.edu.tr

Abstract. In this work, the optical CCD observations and long slit spectra of the galactic supernova remnants G59.5+0.1, G84.9+0.5 and G67.7+1.8 are presented. The observations are carried out with the RTT150 1.5 m -Russian-Turkish joint Telescope, at TUBİTAK National Observatory (TUG) in Antalya, Turkey. The optical observations of G59.5+0.1 and G84.9+0.5 are reported here as the first observations of these supernova remnants. The images are taken with Hα, [SII] and their continuum filters. After subtracting the continuum from Hα. and [SII], [SII]/Hα ratio is obtained. This average ratio is found to be 0.41 and 0.44 for G59.5+0.1 G84.9+0.5,respectively which is in a very good agrement with the ratio obtained from the optical spectra of our observations, i.e. 0.46 and 0.40, respectively, indicating that these remnants are close to, or interacting with, HII regions. G59.5+0.1 and G84.9+0.5 remnants are found to show diffuse-shell morphology while G67.7+1.8 showed arc-shell morphology. From the emission lines of the spectra, the electron density Ne, pre-shock density nc, explosion energy E, interstellar extinction E(B-V) and neutral hydrogen column density N(HI) are calculated and presented here while the shock velocity Vs is also estimated from our observations.

1. INTRODUCTION

Supernova remnants (SNRs) are one of the most important objects of the intergalactic medium. They are located in the galactic plane where the density of gas and dust is very high and their distance from the galactic plane are not larger than 100 pc. Most of the SNRs are observed in radio and x-ray bands. There are 265 SNRs reported in Green (2006) catalog and, because of the very strong interstellar ex-

tinction in their line of sight, very few of them are observed in optical band. However, some of the nearest and least-absorbed ones can be observed on deep exposures with narrow-band filters centered on characteristic emission lines. Photometric and spectroscopic observations performed in optical band give information about the properties of the interstellar medium and the remnant itself, such as the electron density of the medium, pre-shock cloud density and explosion energy (Osterbrock 1989).

The aim of this work is to test whether diffuse objects like SNRs can be observed with Russian-Turkish Telescope (RTT150)+TFOSC (Turkish Faint Object Spectrograph and Camera). The sources selected for observation are G27.4+0.0, G28.6-0.1, G29.6+0.1, G31.9+0.0, G33.6+0.1, G39.2-0.2, G41.1-0.3, G43.3-0.2, G57.2+0.8, G59.5+0.1, G67.7+1.8, and G84.9+0.5, majority of which have no optical observations. Test observations of this sources were obtained with Hα and Hα continuum filters with 300 s exposure times. Under these circumstances, were able to detect optical radiation in from only G59.5+0.1, G84.9+0.5, and G67.7+1.8.

2. OBSERVATIONS

2.1. Optical Images

The 12 SNRs chosen for optical study were observed at the Cassegrain focus of the RTT150+TFOSC (2048×2048 pixel, 15μm × 15μm/ pixel) (more information can be obtained from www.tug.tubitak.gov.tr/tug summary.html).

The sources selected for observation are G27.4+0.0, G28.6-0.1, G29.6+0.1,G31.9+0.0, G33.6+0.1, G39.2-0.2, G41.1-0.3, G43.3-0.2, G57.2+0.8, G59.5+0.1, G67.7+1.8, and G84.9+0.5, 11 of which have no optical observations. To make comparison of our observations we selected G67.7+1.8 which was first observed by Mavromatakis *et al*. (2001).

Table 1. Information of observations.

Filter	Wavelength	Obs. Date (UT)			Exp. times (s)
	(FWHM) (Å)	G59.5+0.1	G84.9+0.5	G67.7+1.8	(no. of frames)
Hα	6563 (88)	28-29 August 2005	6-7 July 2005	7 July 2005	300 (5)
Hα cont.	6446 (130)	28-29 August 2005	6-7 July 2005	7 July 2005	300 (5)
SII	6728 (70)	28-29 August 2005	6-7 July 2005	7 July 2005	300 (5)
SII cont	6964 (300)	28-29 August 2005	6-7 July 2005	7 July 2005	300 (5)

Test observations of these sources were obtained with Hα and Hα continuum filters with 300 s exposure times. Under these circumstances, were able to detect optical radiation in from only G59.5+0.1, G84.9+0.5, and G67.7+1.8. Further optical images, as well as optical spectra, were obtained only of these three sources. The optical images were obtained with the interferences filters Hα, Hα continuum, [SII] and [SII] continuum. The information of observations is given in the Table 1.

2.1.1. [SII]/Hα image of G59.5+0.1, G67.7+1.8 and G84.9+0.5

Dividing the [SII]-[SII]continuum with Hα-Hα continuum images with IRAF imarith package, [SII]/Hα images of these sources were obtained.

[SII]/Hα ratio was obtained for several different locations in each remnant, as indicated by the little boxes on the image.

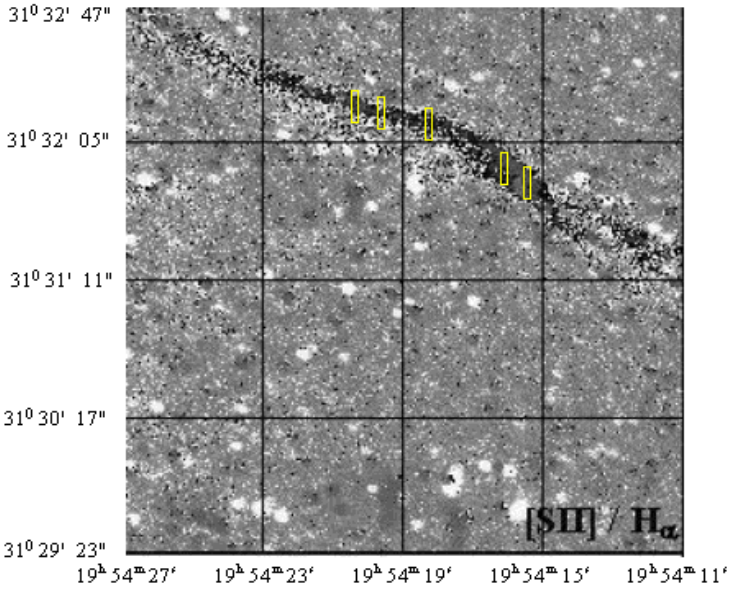

Figure 1: The negative of the [SII]/Hα image of G 67.7 + 1.8 . The image has been smoothed to suppress the residuals from the imperfect continuum substraction. The little boxes shows the places where [SII]/Hα is obtained.

Table 2. [SII]/Hα ratios and their errors for different regions of the G67.7+1.8.

Area	Coordinates J(2000)	[SII]/Hα
1	$\alpha=19^h\ 54^m\ 20^s.25$, $\delta=31^0\ 32'\ 15"$	0.6 (±0.1)
2	$\alpha=19^h\ 54^m\ 19^s.40$, $\delta=31^0\ 32'\ 13"$	0.7 (±0.1)
3	$\alpha=19^h\ 54^m\ 18^s.20$, $\delta=31^0\ 32'\ 11"$	0.7 (±0.2)
4	$\alpha=19^h\ 54^m\ 16^s.20$, $\delta=31^0\ 31'\ 55"$	0.7 (±0.2)
5	$\alpha=19^h\ 54^m\ 15^s.40$, $\delta=31^0\ 31'\ 40"$	0.8 (±0.1)

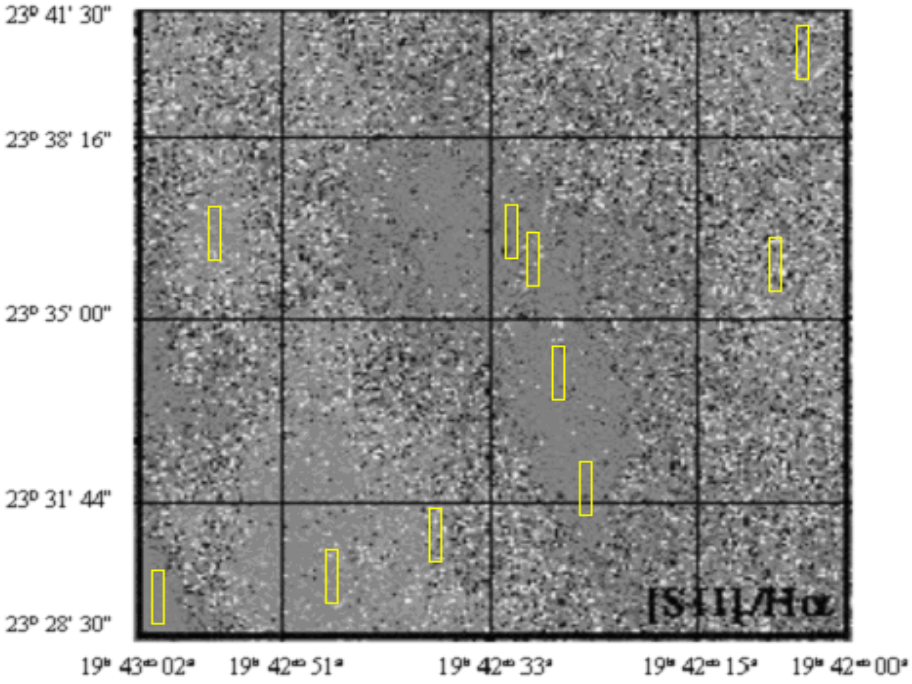

Figure 2: The negative of the [SII]/Hα image of G59.5+0.1. The image has been smoothed to suppress the residuals from the imperfect continuum substraction. The little boxes show the places where [SII]/Hα ratio is calculated.

Table 3. [SII]/Hα ratios and their errors for different regions of the G59.5+0.1.

Area	Coordinate J(2000)	[SII]/Hα
1	$\alpha=19^h\,43^m\,01^s$, $\delta=23^0\,29'\,20''$	0.5 (±0.1)
2	$\alpha=19^h\,42^m\,57^s$, $\delta=23^0\,36'\,35''$	0.3 (±0.2)
3	$\alpha=19^h\,42^m\,48^s$, $\delta=23^0\,29'\,52''$	0.3 (±0.1)
4	$\alpha=19^h\,42^m\,38^s$, $\delta=23^0\,31'\,18''$	0.4 (±0.1)
5	$\alpha=19^h\,42^m\,31^s$, $\delta=23^0\,36'\,43''$	0.5 (±0.1)
6	$\alpha=19^h\,42^m\,30^s$, $\delta=23^0\,36'\,11''$	0.5 (±0.2)
7	$\alpha=19^h\,42^m\,28^s$, $\delta=23^0\,34'\,03''$	0.6 (±0.2)
8	$\alpha=19^h\,42^m\,25^s$, $\delta=23^0\,32'\,05''$	0.6 (±0.1)
9	$\alpha=19^h\,42^m\,08^s$, $\delta=23^0\,36'\,01''$	0.2 (±0.1)
10	$\alpha=19^h\,42^m\,05^s$, $\delta=23^0\,39'\,48''$	0.2 (±0.2)

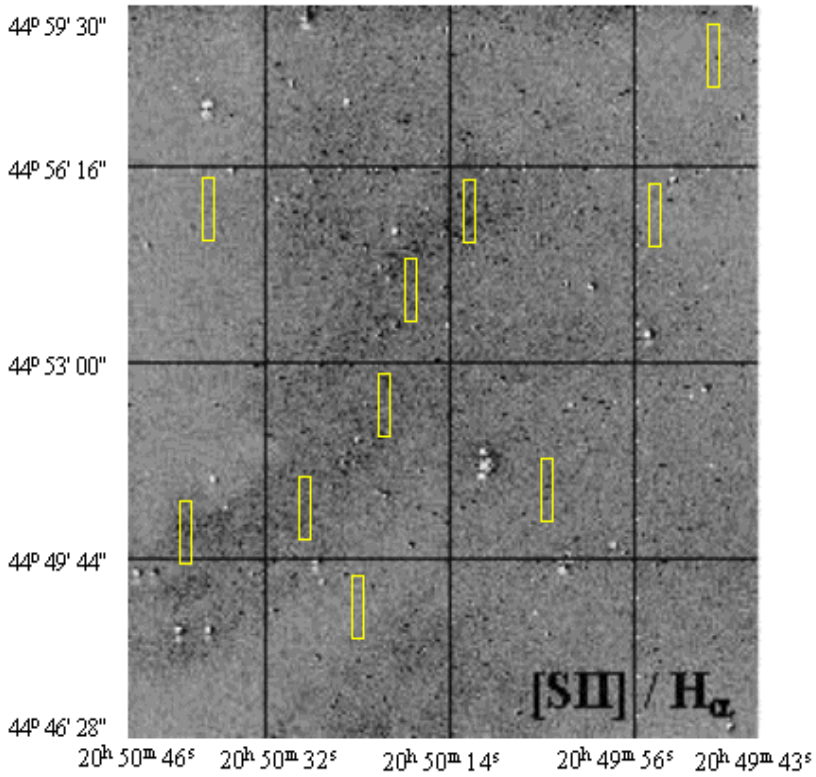

Figure 3: The negative of the [SII]/Hα image of G84.9+0.5 The image has been smoothed to suppress the residuals from the imperfect continuum substraction. The little boxes show the places where [SII]/Hα ratio is calculated.

Table 4. [SII]/Hα ratios and their errors for different regions of the G84.9+0.5.

Area	Coordinate J(2000)	[SII]/Hα
1	$\alpha=20^h\ 50^m\ 40^s$, $\delta=44^0\ 50'\ 30"$	0.6 (±0.1)
2	$\alpha=20^h\ 50^m\ 37^s$, $\delta=44^0\ 55'\ 25"$	0.3 (±0.1)
3	$\alpha=20^h\ 50^m\ 28^s$, $\delta=44^0\ 50'\ 45"$	0.5 (±0.1)
4	$\alpha=20^h\ 50^m\ 23^s$, $\delta=44^0\ 48'\ 33"$	0.3 (±0.1)
5	$\alpha=20^h\ 50^m\ 20^s$, $\delta=44^0\ 52'\ 35"$	0.6 (±0.1)
6	$\alpha=20^h\ 50^m\ 18^s$, $\delta=44^0\ 54'\ 25"$	0.5 (±0.1)
7	$\alpha=20^h\ 50^m\ 12^s$, $\delta=44^0\ 55'\ 20"$	0.7 (±0.1)
8	$\alpha=20^h\ 50^m\ 05^s$, $\delta=44^0\ 51'\ 20"$	0.3 (±0.1)
9	$\alpha=20^h\ 49^m\ 54^s$, $\delta=44^0\ 55'\ 18"$	0.2 (±0.1)
10	$\alpha=20^h\ 49^m\ 47^s$, $\delta=44^0\ 58'\ 45"$	0.4 (±01)

2.1.2. Conclusions of Phometric Observations

From the optical images obtained in our observations using the Hα filter, it can be clearly seen that the SNRs G59.5+0.1 and G84.9+0.5 have diffuse-shell while the remnant G67.7+1.8 has arc-shell morphology.

The [SII]/Hα ratio obtained by optical imaging is found to be 0.41 and 0.44 for G59.5+0.1 and G84.9+0.5, respectively. (Theoretical models generally predict [SII]/Hα ratios to be in the range of 0.5-1.0 for SNRs (Raymond 1979; Shull and McKee 1979) in HII regions and the [SII]/Hα ratio is expected to be $0.1 - 0.3$ (Osterbrock 1989)).

These values imply that photoionization of the gas is dominant. In other words, SNRs G59.5+0.1 and G84.9+0.5 are close to, or interacting with, HII regions. In fact, the radio observations performed by Lockman (1989) reveal that there is an HII region in the neighborhood of G59.5+0.1.

The [SII]/Hα ratio obtained by optical imaging is found to be 0.70 for G67.7+1.8. Accordingly, one can say that in this region collisional ionization of the gas is dominant. On the other hand, there is no observational information if there is any HII region in the neighborhood of G67.7+1.8.

2.2. Optical Spectra

The long-slit spectra were obtained, almost simultaneously with the photometric observations, with the spectroscopic mode of the TFOSC attached to Cassegrain focus of the RTT150. The slit width was 134 μm. The grism used is in the wavelength range of 3870 °A - 6805 °A.

Table 5. Information of the spectroscopic observations.

SNR	Area I Slit Center (J2000)	Area II Slit Center (J2000)	Exposure Time (s)	No. of Frames
G 59.5+0.1	$\alpha=19^h\ 42^m\ 33^s$	$\alpha=19^h\ 42^m\ 25^s$	900	3
	$\delta=23^0\ 36'\ 18''$	$\delta=23^0\ 32'\ 25''$		
G67.7+1.8	$\alpha=19^h\ 54^m\ 16^s$	$\alpha=19^h\ 54^m\ 20^s$	900	3
	$\delta=31^0\ 31'\ 50''$	$\delta=31^0\ 32'\ 14''$		
G 84.9+0.5	$\alpha=20^h\ 50^m\ 16^s$	$\alpha=20^h\ 50^m\ 23^s$	900	3
	$\delta=44^0\ 55'\ 03''$	$\delta=44^0\ 53'\ 00''$		

2.2.1. The long slit spectra of G59.5+0.1, G67.7+1.8 and G84.9+0.5

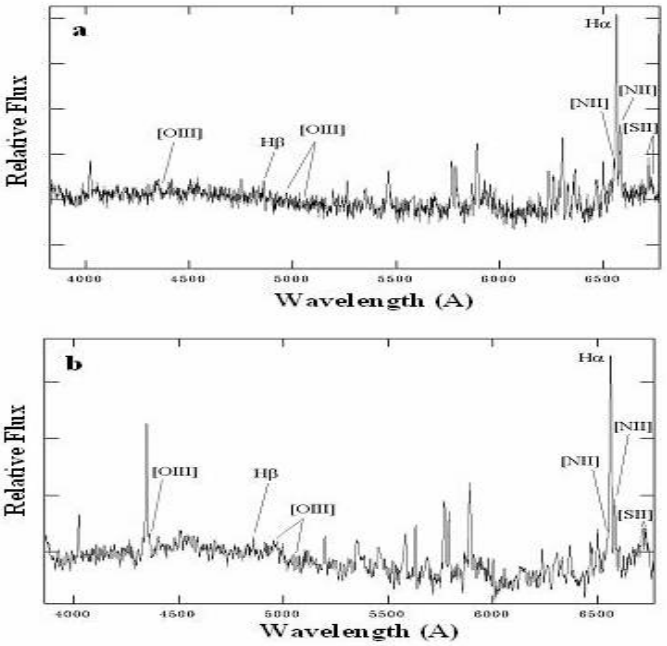

Figure 4: The long slit spectra of G59.5+0.1 for area 1 (a) and area 2 (b).

Table 6. Line fluxes and the parameters obtained from spectra for two different areas of the G59.5+0.1.

Lines (Å)	Flux (F(Hα)=100)		Parameters	Values	
	Area 1	Area 2		Area 1	Area 2
4861 Hβ	14 (2)	8 (1)	[SII][a] / Hα	0.46	0.45
4959 [OIII]	13 (1)	14 (1)	[SII]λ6716/6731	1.19	1.04
5007 [OIII]	12 (1)	13 (1)	Ne (cm^{-3})	313	585
6548[NII]	23 (2)	21 (2)	Vs (km s^{-1})	80	80-100
6563 Hα	100 (10)	100 (9)	n_e (cm^{-3})	11	16
6584[NII]	47 (4)	34 (3)	E (erg)	$0.7x10^{50}$	$1.4x10^{50}$
6716 [SII]	25 (3)	23 (2)	E(B-V)	0.76	1.24
6731 [SII]	21 (1)	22 (2)	Av	2.36	3.84

[a] [SII] is the combination of λ6716 and λ6731 flux values. Numbers in parentheses represent the signal to noise ratio.

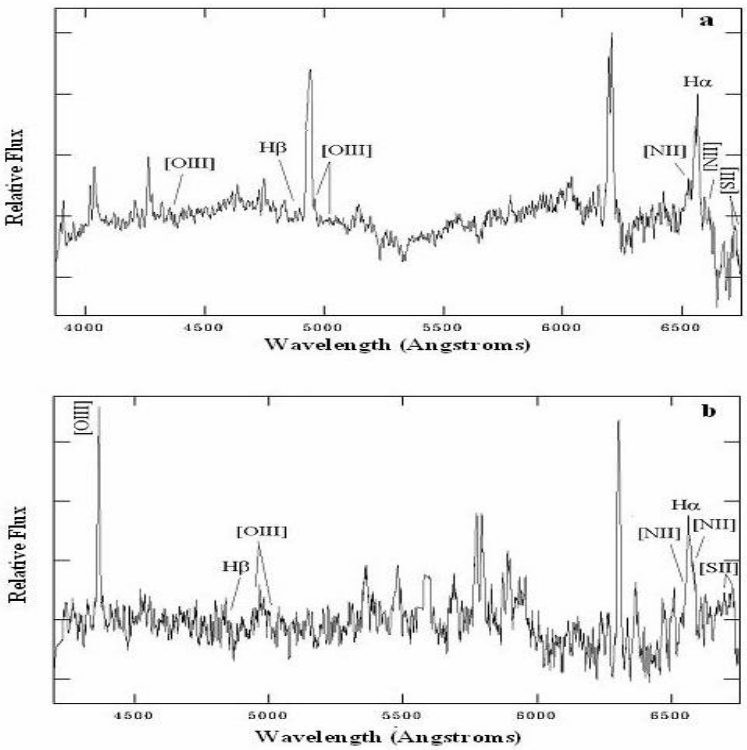

Figure 5: The long slit spectra of G67.7+1.8 for area 1 (a) and area 2 (b).

Table 7. Line fluxes and the parameters obtained from spectra for two different areas of the G67.7+1.8.

Lines (Å)	Flux (F(Hα)=100)		Parameters	Values	
	Area 1	Area 2		Area 1	Area 2
4861 Hβ	13 (1)	23 (1)	[SII][a]/ Hα	0.80	0.71
4959 [OIII]	38 (3)	42 (2)	[SII]λ6716/6731	1.16	1.09
5007 [OIII]	12 (1)	35 (1)	Ne (cm^{-3})	358	480
6548[NII]	55 (7)	49 (3)	Vs (km s^{-1})	80	80-100
6563 Hα	100 (11)	100 (7)	n_e (cm^{-3})	12	13
6584[NII]	50 (3)	68 (2)	E (erg)	$9.3x10^{50}$	$12.8x10^{50}$
6716 [SII]	43 (4)	37 (4)	E(B-V)	0.82	0.32
6731 [SII]	37 (3)	34 (3)	Av	2.54	0.99
			N(HI) (cm^{-2})	$0.4x10^{22}$	$0.2x10^{22}$

[a] [SII] is the combination of λ6716 and λ6731 flux values. Numbers in parentheses represent the signal to noise ratio.

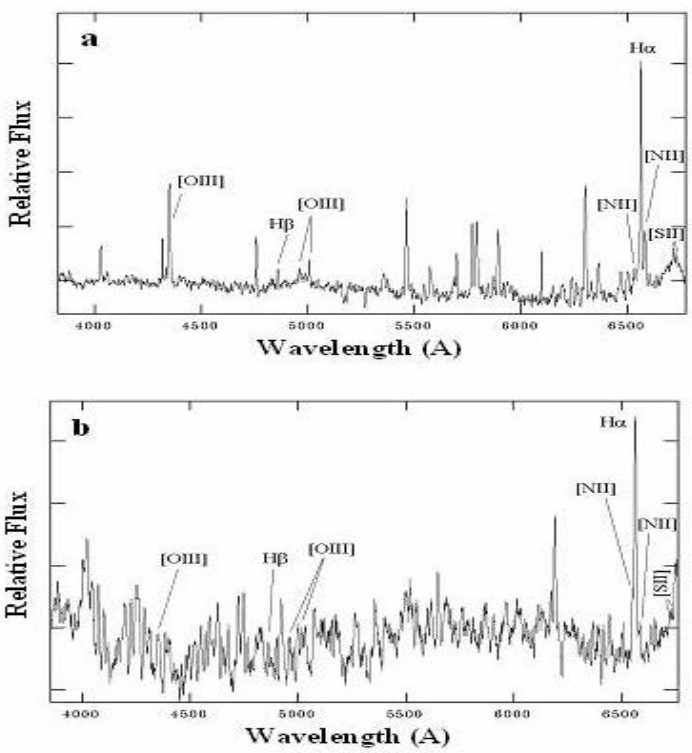

Figure 6: The long slit spectra of G84.9+0.5 for area 1 (a) and area 2 (b).

Table 8. Line fluxes and the parameters obtained from spectra for two different areas of the G 84.9+0.5

Lines (Å)	Flux (F(Hα)=100)		Parameters	Values	
	Area 1	Area 2		Area 1	Area 2
4861 Hβ	7 (2)	11 (1)	[SII][a]/ Hα	0.38	0.41
4959 [OIII]	8 (2)	23 (1)	[SII]λ6716/6731	1.24	1.16
5007 [OIII]	18 (3)	27 (2)	Ne (cm^{-3})	244	358
6548[NII]	10 (1)	12 (1)	Vs ($km\ s^{-1}$)	80-100	80-100
6563 Hα	100 (22)	100 (5)	n_e (cm^{-3})	7	10
6584[NII]	28 (5)	21 (1)	E (erg)	$0.8x10^{50}$	$1.1x10^{50}$
6716 [SII]	21 (2)	22 (1)	E(B-V)	1.36	0.96
6731 [SII]	17 (2)	19 (2)	Av	4.22	2.98
			N(HI) (cm^{-2})	$0.7x10^{22}$	$0.5x10^{22}$

[a] [SII] is the combination of λ6716 and λ6731 flux values. Numbers in parentheses represent the signal to noise ratio.

First of all we should say that these remnats are at the faint edge of RTT150, so the emission lines are weak, that is to say, signal to noise ratio is low. The results obtained in this work may be regarded as approximate values.

Assuming typical electron temperature 10^4 K for gaseous nebula, we estimated basic SNR parameters.

The electron density is calculated through [SII]J(λ6716/λ6731) flux ratio (Osterbrock 1989).

Shock velocity is estimated from the ratio [OIII]λ5007/Hα (Cox and Raymond 1985, Raymond *et al.* 1988, Hartigan *et al.* 1987). Pre-shock cloud density is calculated using the equation of (Fesen and Kirshner 1980)

$$n[SII] = 45 n_c \, (V_S/100)^2 \text{ cm-3}$$

where n[SII] is the density calculated using the [SII] emission line from the optical spectra.

Shock wave energy is given by the equation of McKee and Cowie (1975)

$$E = 2 \times 10^{46} \beta^{-1} \, nc \, (V_S/100)^2 \, r_S^3 \text{ ergs}$$

where r_S is the radius of the shock wave. The factor is approximately equal to 1 at the blast wave shock.

The interstellar extinction and absorption through the relations of Kaler (1976) and Aller (1984)

$$c = 1/0.331 \log[(H\alpha / H\beta)/3]$$
$$E(B - V) = 0.664c$$
$$Av = 3.1 \times E(B - V)$$

Neutral hydrogen column density is calculated through the relation given by Predehl and Schmitt (1995)

$$N(HI) = 5.4 \times 10^{21} \times E(B - V)$$

2.2.3. Conclusion of spectrometric observations

The observed emission line spectrum of the SNRs contains typical permitted lines of H-alpha, H-beta and forbidden lines of [OIII]λ 4363, λ 4959, λ5007, [SII] λ6716, λ 6731, [NII] λ6548, λ6584. In the spectra of G59.5+0.1, G67.7+1.8, and G84.9+0.1, the lines mentioned above, also show up. Forbidden emission lines appear only in the spectra taken from low electron density regions.

In this work, [SII]λ6716/λ6731 ratio obtained from the spectra ranges from 1.04 to 1.24. We have calculated the electron density of G59.5+0.1 ranging between 313 and 585 cm^{-3}, however this value ranges between 244 and 358 cm^{-3} for G84.9+0.1, and for G67.7+1.8 it is in the range (358-480) cm^{-3}. Theoretical

models predict that the electron density in a SNR should be in the range of 10^2-10^4 cm^{-3}, as have been indicated by Osterbrock (1989).

The first optical observation of G67.7+1.8 was made by Mavromatakis *et al.* (2001) and they obtained [SII]/Hα =1,2 (±0,1), [SII] (λ 6716/λ 6731) = 1,28(±0, 08), Ne 142 cm-3, Vs = 70 km/s, E(B − V) = 1.7(±0.3). However, Mavromatakis *et al.* (2001) do not mention about the spectra of the remnant and the slit coordinate of the spectra. Therefore, their results can not be compared one by one. Nevertheless, we can say that our results are in reasonable agreement with theirs.

Acknowledgments

This work is supported by the Akdeniz University Scientific Research Project Management, under project code 2004.03.0121.013. A.S. is supported by TUBITAK Post-Doctoral Fellowship. We would like to thank TUG (TUBITAK National Observatory) for providing us the observations that took place under the project code TUG-RTT150.08.35. We are grateful to Prof. Fotis Mavromotakis of the University of Crete, Physics Department, for his useful comments via e-mail throughout this work.

References

Aller, L. H.: 1984, Physics of thermal gaseous nebulae, D. Reidel Publishing.
Cox, D. P., Raymond, J. C.: 1985, *Astrophys. J.*, **298**, 651.
Fesen, R. A., Kirshner, R. P.: 1980, *Astron. J.*, **242**, 1023.
Frank, J., King, A., Raine, D.: 2002, *Accretion Power in Astrophysics*, Cambridge University Press, Cambridge, NewYork.
Green, D. A.: 2006, *A Catalogue of galactic Supernova Remnants*, http://www.mrao.cam.ac.uk/surveys/snrs.
Hartigan, P., Raymond, J. C., Hartmann, L.: 1987, *ApJ*, **316**, 323.
Kaler, J. B.: 1976, *ApJS*, **31**, 517.
Lockman, F. J.: 1989, *ApJS*, **71**, 469.
Mavromatakis, F., Papamastorakis, J., Ventural, J.: 2001, *Astron. Astrophys.*, **370**, 265.
McKee, C.F., Cowie, L.L.: 1975, *ApJ*, **195**, 715.
Osterbrock, L. H.:1989, *Astrophysics of Gaseous Nebulae and Active Galactic Nuclei.*, California University Press, California.
Predehl, P., Schmitt, J. H. M. M.: 1995, *Astron. Astrophys.*, **293**, 889.
Raymond, J. C.: 1979, *ApJS*, **39**, 1.
Raymond, J. C., Hester, J. J., Cox, D., Blair, W. P., Fesen, R. A., Gull, T. R.: 1988, *ApJS*, **324**, 869.
Shull, J. M., McKee, C. F.:1979, *ApJ*, **227**, 131.